JOURNAL OF SOLID STATE CHEMISTRY 103, 208–215 (1993)

Electrical and Magnetic Properties of Some Mixed $Ln^{III}O_xN_{1-x}$ Phases

GUO LIU,* X. CHEN, AND H. A. EICK†

Department of Chemistry and Center for Fundamental Materials Research, Michigan State University, East Lansing, Michigan 48824-1322

Received March 17, 1992; in revised form August 26, 1992; accepted September 1, 1992

Some pseudobinary and pseudoternary oxidenitrides (CeN–CeO_2; LaN–Ln_2O_3; CeN–Ln_2O_3, Ln = La, Y; and YN–Ln_2O_3, Ln = La, Lu, Y, Sc) were prepared in Ta, Nb, or Mo containers at temperatures between 1500 and 1800°C and characterized by X-ray powder diffraction. Electrical and magnetic properties of two oxidenitrides, $LaO_{0.31}N_{0.69}$ (I) and $LaO_{0.45}N_{0.55}$ (II), were determined over the temperature range 2–300 K. Both are weakly paramagnetic and metallic. Room temperature (300 K) resistivities for I and II are 4.8×10^{-3} and 5.9×10^{-5} Ω cm, respectively. As the temperature is lowered, resistivities of LaO_xN_{1-x} initially decrease linearly. © 1993 Academic Press, Inc.

Introduction

Structure–composition relationships have been reported for the NaCl-type oxidenitride systems, LnO_xN_{1-x}, Ln = La–Er, except Pm, Gd, and Dy (*1–3*). In most systems the cubic nitride lattice parameter is reported to decrease almost linearly as oxygen content increases. Magnetic and electrical transport properties of some of these compounds, principally NdO_xN_{1-x} and the Eu-related systems, $Eu^{2+}_{1-x}Ln^{3+}_xO_{1-x}N_x$ (Ln = Nd, Eu, Gd) (*4–6*), have been studied extensively as a function both of composition and of temperature. The NdO_xN_{1-x} phases are ferromagnetic and metallic. Conductivity increases with increasing oxide content and resistivities vary from 10^{-3} Ω cm for x = 0.09 to 10^{-4} Ω cm for x = 0.22. The transport properties of $Eu_{1-x}Ln_xO_{1-x}N_x$ compounds differ from those of the NdO_xN_{1-x} analogues. The oxygen-rich $Eu_{1-x}Ln_xO_{1-x}N_x$ oxidenitrides for Ln = Gd, Eu are ferromagnetic semiconductors; that for Ln = Nd is a ferrimagnetic semiconductor. The nitrogen-rich specimens are metallic. Europium is found in both the +2 and +3 oxidation states. Magnetic properties are closely related to the predominantly localized *f* electrons.

Since La^{3+} has no unpaired electrons, the LaO_xN_{1-x} oxidenitrides should differ from the systems mentioned above. Both LaN and LaO have the NaCl-type structure (*7–9*). The conductivity of LaN is probably that of a small band overlap semimetal (*10*). Superconductivity has been reported for LaN with a transition temperature of 1.35 K (*11*). LaO prepared under high pressures is metallic and the La ion trivalent (*9*); it is better formulated as $La^{III}(O,e)$, where *e* rep-

---

* Present address: Institute for Materials Research, McMaster University, Hamilton, Ontario Canada L8S 4M1.

† To whom correspondence should be addressed.

0022-4596/93 $5.00

resents a free electron. Since $La^{III}(O,e)$ is reported to be soluble in LaN to the ~45 mole% level (*1*), substitution of oxygen for nitrogen in LaN was expected to enhance its conductivity by increasing the electron carrier density. We synthesized numerous oxidenitride phases in which the La was partially or completely replaced by Group 3 elements devoid of unpaired electrons and measured the magnetic properties of all specimens in the 2–10 K temperature range and the electrical and magnetic properties of two LaO_xN_{1-x} specimens over the 2–300 K temperature range. We report the results of these studies.

Experimental

The *Ln*N compounds, *Ln* = La, Ce, and Y, were prepared from *Ln* chips (>99.5% pure, Research Chemicals, Phoenix, AZ) confined in Al_2O_3 crucibles and heated in flowing $NH_3(g)$ (Matheson) at 700°C for 12 hr (900°C for Y; lower temperatures yielded YH_2). The LaN contained ~5% La_2O_3, the CeN ~10% CeO_2, and the YN ~20% Y_2O_3 as well as ~5% YH_2. Oxidenitride specimens were prepared by grinding intimately *Ln*N–oxide mixtures, confining them in closed 6 mm i.d. Ta, Nb, or Mo tubes, heating them inductively for 2–3 hr *in vacuo* at 1500–1800°C, and quenching them. The LaN–Ln_2O_3 mixed compositions, which typically were heated at 1500–1550°C, are indicated in Table I; the CeN and YN mixed compositions and their synthesis temperatures are presented in Table II. The two La(O,N) specimens that were examined in detail were synthesized from mixtures that contained ~7.0 (I) and ~12 mole% (II) La_2O_3. The products, sintered rods ~4 mm o.d. and 6–8 mm long, were used as synthesized for resistance measurements, but crushed for magnetic and X-ray characterization. Samples were manipulated in an argon-filled glove box whose moisture and oxygen content were typically <3 and 2000–3000 ppm_v, respectively, for the LaN specimens, but the moisture content ranged to ~30 ppm, for the CeN and YN specimens. The nitrides and oxidenitrides are moisture sensitive.

Direct current resistances of I and II were measured with a four probe arrangement on a Quantum Design SQUID magnetometer from 2–300 K; copper wires were spot-welded to the samples. To eliminate the thermal emf contribution to the voltage readings measurements were performed with positive and reversed polarities for 20 sec each and then averaged. Resistivity errors are estimated to be less than 5% and resulted principally from inaccuracies in the size measurement of the irregular-shaped specimens. Magnetic susceptibilities of I and II were also measured with the SQUID from 2–300 K at various magnetic fields between 200 and 20000 G. A diamagnetism correction was applied to the susceptibilities of I and II as described by Selwood (*12*) and the susceptibilities were extrapolated to zero reciprocal field. The magnetic susceptibilities of all other specimens were measured typically from 2 to 10 K, at 200 and at 20 G to check for superconductivity. The magnetic susceptibility of one specimen to which elemental La had been added was also determined.

Powder X-ray diffractograms were determined with a 114.59 mm diameter Guinier camera with monochromated Cu$K\alpha_1$ radiation ($\lambda\alpha_1$ = 1.54050 Å) and NBS certified silicon (a = 5.43082(4) Å) as internal standard as described previously (*13*).

Results and Discussion

Phases observed. I and II were cubic single-phase products; reflections assignable to neither elemental La nor to La_2O_3 were observed in the X-ray powder diffraction patterns. I was dark blue while II was deep red; similar colors were reported by Brown and Clark (*1*) for La(O,N) phases.

TABLE I

MIXED COMPOSITION, LATTICE PARAMETER, AND IMPURITY PHASE DATA FOR SOME LANTHANUM-CONTAINING OXIDENITRIDES SYNTHESIZED IN Ta CONTAINERS UNLESS INDICATED OTHERWISE

Mixed composition (mole% Ln_2O_3)		Oxidenitride	a (Å)	T_c (K)	M. F.[a]	Comment
LaN− 7.0%	La_2O_3	$LaO_{0.31}N_{0.69}$	5.2540(5)	6	0.09%, 2 K	pure
LaN−12.2%	La_2O_3	$LaO_{0.45}N_{0.55}$	5.2273(8)	6	4.2%, 2 K	pure
LaN−38.%	CeO_2	$La_{0.85}Ce_{0.15}$(O,N)	10.4161(8)	—		pure
LaN− 7.7%	Lu_2O_3	(La,Lu)(O,N)	5.2230(5)	—		La_2O_3(T), ~50% LuO_xN_{1-x}
LaN−14.%	Y_2O_3	$La_{0.79}Y_{0.21}$(O,N)	5.1456(3)	6[c]	49.5%, 5 K	~10% $(La,Y)_2O_3$
LaN− 7.4%	Y_2O_3	$La_{0.87}Y_{0.13}$(O,N)	5.1579(4)	—		~5% $(La,Y)_2O_3$
LaN− 6.8%	Sc_2O_3	unidentified[b]		6	12%, 5 K	La_2O_3 (major)
LaN− 7.4%	Y_2O_3	(La,Y)(O,N)	5.2160(5)	6[a,d1]		Mo container
LaN−14.%	Y_2O_3	(La,Y)(O,N)	5.1553(7)	6[a,d2]		Mo container
La ——				6		
LaN− 7.4% La	Y_2O_3 }			6		La chips added to oxidenitride

[a] Meissner fraction; varied from sample to sample.

[b] Ten reflections indexed by (*18*) with $a = 14.527(7)$, $b = 7.327(1)$, $c = 5.680(1)$ Å; $M(10) = 12$.

[c] Unassigned X-ray diffraction reflections: 3.375 (vw), 3.270 (vw), 3.046 (w), and 2.263 Å (vs). The first can be assigned to TaO (3.371 Å, (100, relative intensity)) (*19*). Although the second and third reflections correspond to the 3.29 Å (60) and 3.04 Å (100) values for α-La, the 2.86 Å (80) spacing is absent (*20*). A similar situation prevails for the high temperature (hexagonal) form of Y_2O_3 (*21*). The phase responsible for these reflections could not be identified.

[d] Unassigned X-ray diffraction reflections: $d1$: $d = 6.039$ and 5.215 Å; $d2$: $d = 5.968$ and 5.177 Å.

The nitrogen content of these specimens was deduced from a least-squares fit of the published LaO_xN_{1-x} nitrogen composition–lattice parameter data (*1*); synthesis conditions used in this work were similar to those reported in (*1*). The formulas derived for I and II are $LaO_{0.31}N_{0.69}$ and $LaO_{0.45}N_{0.55}$, respectively. In the LaO_xN_{1-x} study (*1*) the lattice parameter remained invariant at $a \approx 5.223$ Å when $x \geq 0.46$. Specimen II, whose lattice parameter is slightly larger than this value, is presumed to have the maximum oxygen content. Lattice parameters of all the oxidenitrides characterized and formulas of other phases identified in the X-ray diffraction patterns are presented in Table I. (The composition of phases other than I and II was assumed to be close to the mixed composition.) The lattice parameter of (La,Lu)(O,N), $a = 5.2230(5)$ Å, is relatively close to that of $LaO_{0.45}N_{0.55}$, suggestive of minimal Lu solubility. Such a result is not surprising in view of the large size difference between the La^{3+} and Lu^{3+} ions.

Although Ta reduced La-containing specimens well, it was only marginally capable of reducing Y-containing samples. Consequently, elemental Y was added to effect reduction when YN was mixed with Lu_2O_3 and Sc_2O_3.

Both the LaN–CeO_2 and CeN–CeO_2 fired samples possessed a doubled cubic lattice parameter (see Tables I and II) as a result of one extra low-angle reflection. This doubled parameter is difficult to understand; it was not reported in previous Ce(O,N) studies (*2*). However, the lattice parameter change from 10.416 Å to 10.229 Å (Tables I and II) when Ce replaces La in the oxidenitride supports the reflection's being integral to the system.

Upon exposure to the laboratory atmo-

TABLE II

MIXED COMPOSITION, LATTICE PARAMETER, AND IMPURITY PHASE DATA FOR SELECTED OXIDENITRIDES SYNTHESIZED IN Ta CONTAINERS

Mixed composition (weight % Ln_2O_3[a])	Impurity[b]	a (Å)	Reaction temperature (°C); specimen color
YN		4.877	(*22, 23*)
YN – 9.1% Y_2O_3	Y_2O_3(L)	4.8580(1)	1850; brown
YN –17.4% Y_2O_3	Y_2O_3(L)	4.8631(2)	1850; brown
YN – 9.0% Sc_2O_3 3.7% Y	Y_2O_3(T)[c1]	4.818(1)	1700; dk purple
YN –16.4% Sc_2O_3 2.7% Y	Y_2O_3(L)	4.7889(3)	1760; purple
YN – 9.2% Lu_2O_3 3.2% Y	Y_2O_3(T)[c2]	4.8632(5)	1850; dk blue
YN –17.5% Lu_2O_3 3.2% Y	Y_2O_3(L)	4.8526(4)	1760; purple
CeN–25.0% CeO_2	Ce_2O_3(M)	10.229(1)	
CeN– 9.9% Y_2O_3	—[c3]	5.0749(7)	1515; purple-red
CeN–18.0% Y_2O_3	—[c4]	5.0539(6)	1515; purple-red
CeN– 9.9% La_2O_3	—[c5]	5.1182(2)	1500; purple
CeN–18.0% La_2O_3	—	5.1540(4)	1500; purple-blue

[a] Mass Ln_2O_3/total specimen mass. See text regarding addition of Y.

[b] L: significant impurity level; T: trace impurity level.

[c] Unassigned X-ray diffraction reflections: *c*1: d = 5.595 and 4.834 Å; *c*2: d = 5.621 and 4.873 Å; *c*3: d = 5.874 and 5.098 Å; *c*4: d = 5.858 Å; *c*5: d = 5.940 Å.

sphere all products decomposed gradually with evolution of NH_3(g). The X-ray powder diffraction reflections were broad and did not sharpen upon annealing, suggestive of small particle size, inhomogeneous solid solution over a narrow range of compositions, or, less likely, ordered phases with extended cells which formed when the specimens were quenched (*2*). The Ta container which served as the reducing agent was brittle after reaction. However, it separated easily from every specimen except those which contained Sc_2O_3 where melting had occurred, and no more than one X-ray reflection could ever be assigned to a Ta oxide phase. Tantalum is too poor a reducing agent to produce elemental lanthanum during the oxidenitride synthesis, but Ta is known to reduce La_2O_3(*s*) to LaO(g) and be converted to TaO_x(g) and $LaTaO_4$(s) (*14*). After an La_2O_3–14 mole% YN specimen synthesized in a Nb container exhibited a superconducting transition with $T_c \approx 8$ K, suggestive that container impurities were present in the reaction products, nonsuperconducting Mo was used as a container.

Electrical properties of I *and* II. Resistivity–temperature data for I and II are given in Figs. 1 and 2. Room temperature (300 K) resistivities are 4.8×10^{-3} and 5.9×10^{-5} Ω cm, respectively. Both samples exhibit characteristic metallic conductivity in the temperature range 6–300 K. In this normal conducting state the resistivities of both specimens initially decrease linearly as the temperature is lowered. A sharp superconducting transition was observed at $T_c \approx 6$ K for both specimens.

The more oxide-rich $LaO_{0.45}N_{0.55}$ (II) is a better conductor than $LaO_{0.31}N_{0.69}$ (I) in the normal state. At room temperature the resistivity of II is nearly two orders of magni-

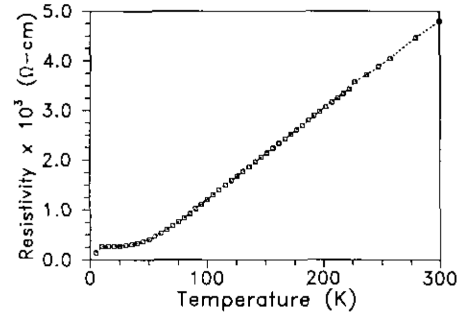

FIG. 1. Plot of $LaO_{0.31}N_{0.69}$ (I) resistivity (Ω cm) against temperature (K).

tude less than that of I, but the thermal coefficient values are reversed. The greater electrical conductivity value of the higher oxygen content specimen suggests that an increase in the oxygen content increases the number of electrons in the conduction band, consistent with the formulation $La^{III}O_x N_{1-x}e_x$. Similar behavior has been observed for NdO_xN_{1-x} (*3*).

Even though resistivities measured on powders are usually greater than those of single crystals, our data on sintered specimens are considered quantitative since grain-boundary resistances should be negligible. The temperature and composition dependencies are well resolved. Based on the deduced compositions, the lattice parameters, and the free electron formulation, electron mobilities can be estimated from the equation $\sigma = ne\mu$, where σ is the conductivity, n the electron density, e the electronic charge, and μ the carrier mobility. Mobilities calculated at 10, 150, and 300 K, respectively, are for I 3.04, 0.376, and 0.168 $cm^2 \cdot V^{-1} \cdot sec^{-1}$, and for II 23.3, 13.4, and 8.39 $cm^2 \cdot V^{-1} \cdot sec^{-1}$. These data suggest that II ($LaO_{0.45}N_{0.55}$) is nearly a free carrier conductor. The reason for the substantially lower mobilities of the less oxygen-rich $LaO_{0.31}N_{0.69}$ is unclear; they may result from the filling of the conduction band only below the mobility edge. However, as is described below, the 4.2% Meissner fraction of $LaO_{0.45}N_{0.55}$ suggests that specimen may contain up to 4% elemental La. Conversely, the negligible Meissner fraction of I suggests a specimen essentially devoid of elemental La, and suggests this lower value more closely corresponds to the conductivity of the pure oxidenitride.

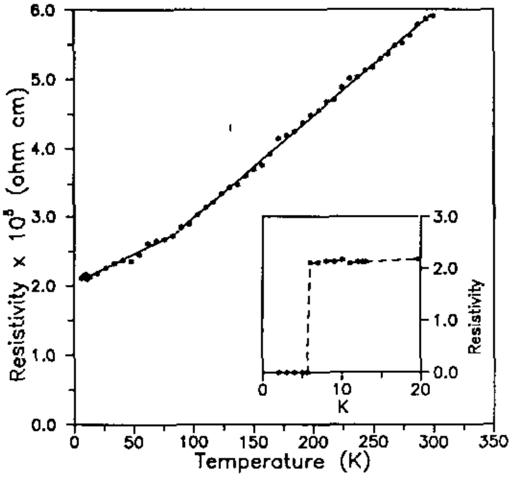

FIG. 2. Plot of $LaO_{0.45}N_{0.55}$ (II) resistivity (Ω cm) against temperature (K). The straight lines represent linear least-squares fits of the data ranges.

Above 6 K the resistivity–temperature plots of both specimens can be described in terms of two linear regions with different slopes. The slopes of the two linear regions intersect at ~50 K for $LaO_{0.31}N_{0.69}$ and ~85 K for $LaO_{0.45}N_{0.55}$, with the thermal coefficients below these temperatures smaller than those above it. The resistivity data for $LaO_{0.45}N_{0.55}$ show more scatter than those for $LaO_{0.31}N_{0.69}$ with a less pronounced break and when the estimated 5% resistivity measurement error is included, the former data can equally well be considered linearly related to temperature, and hence, metallic in character. Any transition that is present is probably related to a structural change, such as an anion ordering as was observed in CeO_xN_{1-x} by electron diffraction (*2*), or a cubic to tetragonal transformation as was

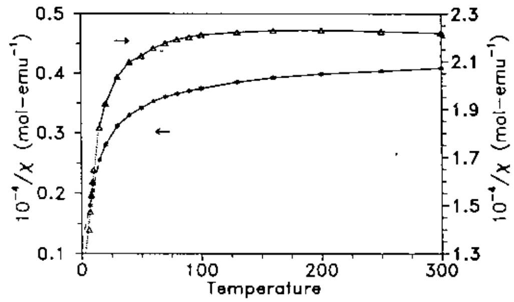

FIG. 3. Graph of the (H_0 = 200 G) inverse molar magnetic susceptibility (mol-emu^{-1}) of II ($LaO_{0.45}N_{0.55}$, *, left axis) and I ($LaO_{0.31}N_{0.69}$, Δ, right axis) against temperature to illustrate Curie–Weiss behavior. The dashed and dotted straight lines represent linear least-squares fits of the low temperature data.

observed for $NdO_{0.06}N_{0.94}$ (*3*). Structural studies—especially neutron or electron diffraction as a function of temperature—must be undertaken to reveal the reason for these changes.

Magnetic properties. The reciprocal molar susceptibilities of I and II are plotted against temperature in Fig. 3 and the susceptibility of II is plotted against temperature in Fig. 4. As the insert in Fig. 4 illustrates, the flux exclusion phenomenon is observed with transition temperatures consistent with those observed in the electrical measurements. At 2 K the Meissner fraction of $LaO_{0.45}N_{0.55}$ (II) is 4.2%; that of $LaO_{0.31}N_{0.69}$ is 0.09%. These data suggest that the superconductivity is produced by a small concentration of impurity phase which we believe to be La metal. The superconductivity cannot be attributed to a Ta impurity, even though Ta was the reductant, because comparable data were obtained with specimens synthesized in nonsuperconducting Mo containers. Elemental lanthanum becomes superconducting below 6 K (*15*) and at the 4% or lower level could not be detected by the Guinier X-ray powder technique. The NH_3(g) synthesis procedure could leave unreacted elemental La encapsulated by nitride in the specimen, but the ensuing reaction with oxide at 1500–1600°C should consume any remaining free element. Additionally, a LaN specimen prepared by reacting the hydride with N_2(g) was not superconducting at 2 K (*15*). Another probable source of elemental La is decomposition of the $LaO_{1-x}N_x$ phase into La(s), a less oxygen-rich La^{III}(e)(O,N)(s) and La_2O_3(s) during the quench, as is indicated in Eq. (1):

$$LaO_{1-x}N_x \rightarrow \left(\frac{x}{x+y}\right) LaO_{1-x-y}N_{x+y} + \frac{y}{3(x+y)} La + \frac{y}{3(x+y)} La_2O_3. \quad (1)$$

Since the Meissner fraction for specimen I was negligible, we presume that preparations more oxygen-rich than I could be quenched without undergoing disproportionation.

The temperature dependence of the magnetic susceptibility of $LaO_{1-x}N_x$ proves the presence of paramagnetic impurities with localized valence electrons. The susceptibility remains almost constant above ~40 K for I and above ~80 K for II, while below these temperatures Curie–Weiss behavior is observed (see Fig. 3). The diamagnetically corrected and zero reciprocal field-extrapolated susceptibilities (χ vs. T) for II are shown in Fig. 5. The nearly constant and small extrapolated susceptibilities in the

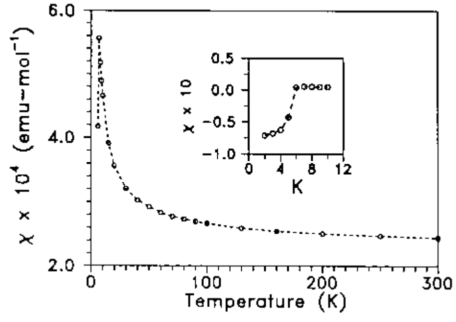

FIG. 4. Plot of the magnetic susceptibility of $LaO_{0.45}N_{0.55}$ (II) against temperature. The onset of flux exclusion at 6 K is illustrated in the insert.

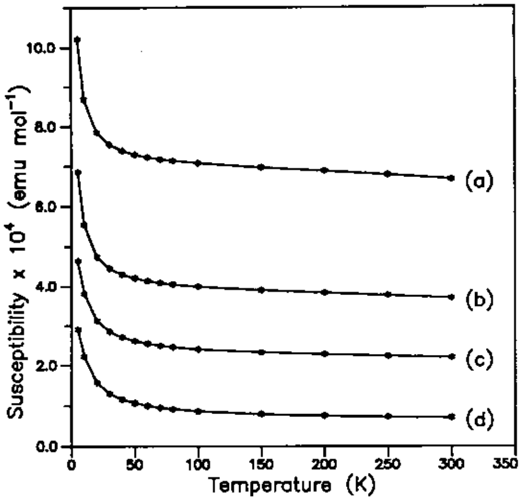

FIG. 5. Temperature dependence of the magnetic susceptibility (emu-mol^{-1}) of II ($LaO_{0.45}N_{0.55}$). Applied magnetic fields are (a) 5000 G; (b) 1 T; (c) 2 T; and (d) extrapolated to infinity.

higher temperature regions are in agreement with a Pauli-type electron gas model of metallic materials. However, the values of 7–10 × 10^{-5} emu · mol^{-1} are significantly larger than expected. The electron densities calculated for the formulation $La^{III}O_xN_{1-x}e_x$ allow the magnetic susceptibility to be estimated from the Pauli–Peierls equation (*16*):

$$\chi = \frac{4m^* \mu_0^2}{h^2}(3\pi^2 n)^{1/3}\left(1 - \frac{m_0^2}{3m^{*2}}\right).$$

In this equation μ_0 is the Bohr magneton of electrons, n the electron density, 7.72 × 10^{21} and 1.26 × 10^{22} electrons · cm^{-3}, respectively, for I and II, m_0 the electronic rest mass, and m^* the effective mass, here taken as m_0. Even neglecting the diamagnetic term ($-m_0^2/3m^{*2}$), with a volume of 21.50 cm^3 · mol^{-1}, the molar Pauli susceptibility for $LaO_{0.45}N_{0.55}$ would be about 1.1 × 10^{-5} emu · mol^{-1}, at least seven times lower than the observed value. The observed high susceptibilities are probably an indication of a narrow $5dt_{2g}$ band structure (*16*).

The magnetic properties of other lanthanoid-substituted lanthanum oxidenitrides $La_{1-x}Ln_x(O,N)$ are summarized in Table I; those of $Y_{1-x}Ln_x(O,N)$ and $Ce_{1-x}Ln_x(O,N)$ are given in Table II. The bulk specimens that were subjected to magnetic analysis were also analyzed by X-ray diffraction; the cubic lattice parameters are listed in the tables. Some spurious interplanar *d*-spacings that could not be assigned to any anticipated phase are also listed. They probably result from trace amounts of unknown quaternary oxidenitride phases. The transition temperature of all the specimens found to be superconducting is essentially the same and only the amount of the superconducting phase varies among preparations, consistent with the superconducting species being elemental La which precipitated during quenching. Superconductivity is not observed for compounds that contain Ln^{3+} ions with *f* electrons, probably because their observed susceptibilities are dominated by the susceptibilities of the *f* electrons.

Metal nitride superconductors with the NaCl-type structure have long been known; NbN has the highest T_c (~18 K) (*17*). The increase of electrical conductivity of the LaO_xN_{1-x} phases with increasing oxygen content appears due to increased electron densities. Further studies on oxidenitrides of different compositions are necessary to determine unequivocally the source of the superconductivity.

Acknowledgment

The assistance of Reza Loloee in obtaining resistivity data is acknowledged gratefully.

References

1. R. C. BROWN AND N. J. CLARK, *J. Inorg. Nucl. Chem.* **36**, 2287–2290 (1974).
2. R. C. BROWN AND N. J. CLARK, *J. Inorg. Nucl. Chem.* **36**, 1777–1782 (1974).
3. C. MOURGOUT, B. CHEVALIER, J. ETOURNEAU, J. PORTIER, P. HAGENMULLER, AND R. GEORGES, *Rev. Hautes Temp. Refract.* **14**, 89–96 (1977), and references therein.

4. B. Chevalier, J. Etourneau, and P. Hagenmuller, *Mater. Res. Bull.* **12,** 473–479 (1977).
5. J. Etourneau, B. Chevalier, P. Hagenmuller, and R. Georges, *J. Phys.* (*Les Ulis, Fr.*) **41,** C5-193–C5-204 (1980).
6. B. Chevalier, J. Etourneau, and P. Hagenmuller, *Rare Earths Mod. Sci. Technol.* **2,** 403–408 (1980).
7. G. L. Olcese, *J. Phys. F* **9,** 569–578 (1979).
8. J. M. Leger, N. Yacoubi, and J. Loriers, *Rare Earths Mod. Sci. Technol.* **2,** 203–208 (1980).
9. J. M. Leger, N. Yacoubi, and J. Loriers, *J. Solid State Chem.* **36,** 261–270 (1981).
10. M. R. Norman, H. J. F. Jansen, D. D. Keolling, and A. J. Freeman, *Solid State Commun.* **52,** 739–741 (1984).
11. J. J. Veyssie, D. Brochier, A. Nemoz, and J. Blanc, *Phys. Lett.* **14,** 261 (1965).
12. P. W. Selwood, "Magnetochemistry," 2nd ed. p. 78, Interscience, New York, (1956).
13. G. Liu and H. A. Eick, *J. Less-Comm. Met.* **156,** 237–245 (1989).
14. P. N. Walsh, H. W. Goldstein, and D. White, *J. Am. Ceram. Soc.* **43,** 229–233 (1961).
15. D. P. Schumacher and W. E. Wallace, *Inorg. Chem.* **5,** 1563–1567 (1966).
16. G. H. Bouchard, Jr., and M. J. Sienko, *Inorg. Chem.* **7,** 441–443 (1963).
17. J. C. Phillips, *Phys. Rev. Lett.* **26,** 543–546 (1971).
18. P. E. Werner, L. Eriksson, and M. Westdahl, *J. Appl. Crystallogr.* **18,** 367–370 (1985).
19. Powder Diffraction File, JCPDS: International Centre for Diffraction Data, 1601 Park Lane, Swarthmore, PA 19801, Data 1983, File No. 34-977.
20. Powder Diffraction File, JCPDS: International Centre for Diffraction Data, 1601 Park Lane, Swarthmore, PA 19801, Data 1983, File No. 2-0618.
21. Powder Diffraction File, JCPDS: International Centre for Diffraction Data, 1601 Park Lane, Swarthmore, PA 19801, Data 1983, File No. 20-1412.
22. Powder Diffraction File, JCPDS: International Centre for Diffraction Data, 1601 Park Lane, Swarthmore, PA 19801, Data 1967, File No. 10-221.
23. D. P. Schumacher and W. E. Wallace, *Inorg. Chem.* **5,** 1563–1567 (1966).